An Efficient Simplified Approach for the Nonlinear Buckling Analysis of Frames

Anthony N. Kounadis*
National Technical University of Athens, Greece

In this paper, a simplified but very reliable approach for the nonlinear buckling analysis of frames subjected to either bifurcational or limit-point instability is proposed. This approach, based on slightly modified kinematic continuity conditions, is demonstrated through the buckling analysis of a simple two-bar frame. Numerical solutions, obtained by an accurate nonlinear buckling analysis and two simplifying variants of it, are established for a wide range of values of several parameters. Comparisons of these solutions show the simplicity, speed, and reliability of the buckling approach proposed herein. Moreover, a simple stability criterion is established for a direct determination of critical loads.

Introduction

THE problem of linear bifurcational analysis of plane frames has been discussed extensively by many investigators during the last 50 years. An excellent review on this subject is given by Bleich.[1] However, considerable attention has recently been given to the nonlinear buckling analysis of frames.[2,3] This is due primarily to the need for a precise estimation of the load-carrying capacity of frames sensitive to small initial imperfections. As is known, the presence of imperfections may decrease the load-carrying capacity of a structural system considerably, depending on the shape of the initial postbuckling path. An outstanding contribution to this problem is the initial postbuckling analysis of Koiter[4]; however, it is only applicable to structural systems which in their primary equilibrium state exhibit bifurcational instability. Thus, for the majority of structural systems which lose their stability through a limit point, a complete nonlinear analysis is required for the estimation of their actual load-carrying capacity. Discrepancies in critical loads obtained by Koiter's initial postbuckling analysis and accurate nonlinear buckling analyses have been presented recently by Kounadis et al.,[5] as well as by Simitses and Kounadis.[6] The last reference presents a systematic nonlinear stability analysis applicable to a general frame composed of straight uniform bars rigidly connected to each other. However, in this analysis considerable difficulties arise for establishing numerical solutions for systems with more than three nonlinear equilibrium equations. Thus, an approximate nonlinear buckling analysis leading to reliable results is desirable.

The objective of this investigation is to present an effective and readily employed nonlinear buckling analysis of plane frames associated with the simplest possible nonlinear equations. In effect, the field equations of the present analysis are those of the linear buckling theory of frames, with the unique exception that the kinematic continuity conditions for the joint translational components are slightly modified. The proposed approach has no restrictions on its range of applicability and, despite the simplification of the nonlinear equations, leads to quite accurate results. The effectiveness of this approach is demonstrated through the buckling analysis of a simple two-bar frame for which numerical results are available.

Received Jan. 23, 1984; revision received Oct. 10, 1984.

*Professor.

Nonlinear Buckling Analysis

The buckling analysis that follows assumes geometrically perfect members made from linearly elastic material which may undergo moderate rotations but small strains. If such a member of length ℓ, cross-sectional area A, and moment of inertia I is subjected simultaneously to bending and axial compression, the following elastic energy functional can be written

$$U=\frac{1}{2}\int_0^\ell [EA(u'+\tfrac{1}{2}W'^2)^2+EIW''^2]\,\mathrm{d}\chi \tag{1}$$

where W and u are the lateral deflection and axial displacement of the centerline of the member, respectively, and E is Young's modulus of member material; the prime denotes differentiation with respect to the axial coordinate χ.

Introducing the nondimensionalized quantities $x=\chi/\ell$, $\xi=u/\ell$, $w=W/\ell$, and $\lambda^2=A\ell^2/I$, Eq. (1) is brought in dimensionless form as follows

$$\underset{\sim}{U}=\frac{U\ell}{EI}=\frac{1}{2}\int_0^1 [\lambda^2(\xi'+\tfrac{1}{2}w'^2)^2+w''^2]\,\mathrm{d}x \tag{2}$$

The two-bar frame shown in Fig. 1 is subjected to a compressive force P applied at its joint, eccentric to the centerline of the column. On the basis of relation Eq. (2), the total potential energy of the frame is given by

$$U^T=\frac{1}{2}\int_0^1 [\lambda_1^2(\xi_1'+\tfrac{1}{2}w_1'^2)^2+w_1''^2]\,\mathrm{d}x_1$$
$$+\frac{\mu}{2\rho}\int_0^1 [\lambda_2^2(\xi_2'+\tfrac{1}{2}w_2'^2)^2+w_2''^2]\,\mathrm{d}x_2$$
$$+\beta^2\rho e w_2'(1)+\beta^2\rho\xi_1(1)=0 \tag{3}$$

where $\mu=I_2/I_1$, $\rho=\ell_2/\ell_1$, $\beta^2=P\ell_1^2/EI_1$, and $e=\epsilon/\ell_2$.

The principle of stationary total potential energy leads to the following differential equations[5]

$$\lambda_1^2(\xi_1'+\tfrac{1}{2}w_1'^2)'=0 \tag{4a}$$

$$\lambda_2^2(\xi_2'+\tfrac{1}{2}w_2'^2)'=0 \tag{4b}$$

$$w_1''''-\lambda_1^2[(\xi_1'+\tfrac{1}{2}w_1'^2)w_1']'=0 \tag{4c}$$

$$w_2''''-\lambda_2^2[(\xi_2'+\tfrac{1}{2}w_2'^2)w_2']'=0 \tag{4d}$$

The boundary conditions associated with the last equations are

$$w_1(0) = \xi_1(0) = w_2(0) = 0 \quad (5a\text{-}c)$$

$$w_1(1) = \rho\xi_2(1) \quad (5d)$$

$$\xi_1(1) = -\rho w_2(1) \quad (5e)$$

$$w_1'(1) = w_2'(1) \quad (5f)$$

$$\xi_2'(0) + \tfrac{1}{2} w_2'^2(0) = 0 \quad (5g)$$

$$w_1''(0) = 0 \quad (5h)$$

$$w_2''(0) = 0 \quad (5i)$$

$$w_1''(1) + (\mu/\rho)w_2''(1) + \beta^2\rho e = 0 \quad (5j)$$

$$w_1'''(1) + k^2 w_1'(1) = 0 \quad (5k)$$

$$(\beta^2 - k^2)\rho^2 + \mu w_2'''(1) = 0 \quad (5l)$$

where $k^2 = S\ell_1^2/EI_1$; S is the axial compressive force in the column. Integration of Eqs. (4), by means of conditions Eqs. (5a-c) and (5g-i), yields

$$\xi_1(x_1) = -\frac{k^2}{\lambda_1^2}x_1 - \frac{1}{2}\int_0^{x_1} w_1'^2 dx_1 \quad (6a)$$

$$\xi_2(x_2) = C - \frac{1}{2}\int_0^{x_2} w_2'^2 dx_2 \quad (6b)$$

$$w_1(x_1) = C_1 \sin kx_1 + C_3 x_1 \quad (6c)$$

$$w_2(x_2) = \bar{C}_1 x_2^3 + \bar{C}_3 x_2 \quad (6d)$$

where C_1, $\bar{C}_1$, C_3, $\bar{C}_3$ are integration constants to be determined, and C represents the horizontal displacement of the movable hinge; consequently, $\xi_2(x_2)$ represents the absolute axial displacement which is equal to the relative axial displacement of the bar plus the horizontal displacement of the movable support. As is shown subsequently, the constant C does not influence the nonlinear equilibrium path and, therefore, the critical load. From conditions (5f) and (5l), it is found that

$$C_1 = \rho[k^2 + \beta^2(e-1)]/k^2 \sin k \quad (7a)$$

$$\bar{C}_1 = \rho^2(k^2 - \beta^2)/6\mu \quad (7b)$$

$$C_3 = 0 \quad (7c)$$

$$\bar{C}_3 = \frac{\rho[k^2 + \beta^2(e-1)]}{k \tan k} - \frac{\rho^2(k^2 - \beta^2)}{2\mu} \quad (7d)$$

By means of relations (7) and Eq. (6a), condition (5e) leads to the following nonlinear equilibrium equation[7]

$$\frac{\rho(\beta^2 - k^2)}{3\mu} + \frac{[k^2 + \beta^2(e-1)]}{k \tan k} - \frac{k^2}{\rho^2\lambda_1^2} - \left[\frac{k^2 + \beta^2(e-1)}{2k \sin k}\right]^2\left(1 + \frac{\sin 2k}{2k}\right) = 0 \quad (8)$$

This equation is independent of the constant C and, therefore, of relation (5d).

By solving Eq. (8) numerically with respect to k for different levels of the load β^2 and various values of the parameters λ_1, ρ, μ, and e, one can establish the entire (prebuckling and postbuckling) equilibrium path. Thus, from Eqs. (6a) and (6c) using Eqs. (7a) and (7c), we obtain the following joint displacement components

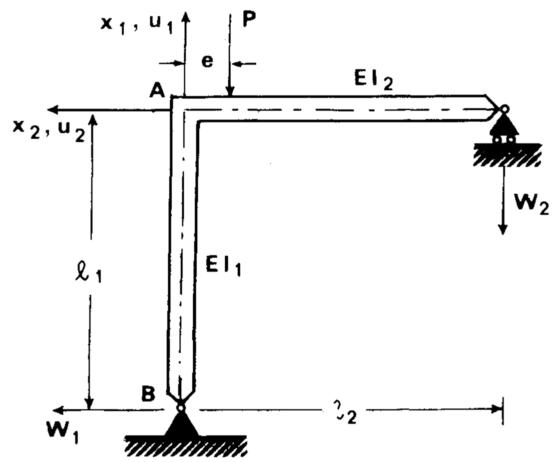

Fig. 1 Geometry and sign convention of a two-bar frame.

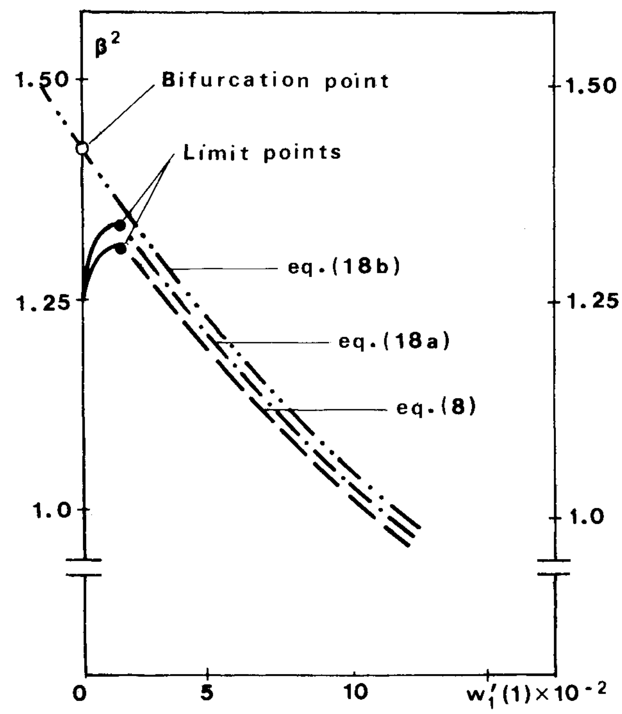

Fig. 2 Equilibrium paths on the basis of the simplified and the accurate nonlinear analysis for $e = 0$, $\lambda_1 = 40$, and $\rho = \mu = 1$.

$$\xi_1(1) = -\frac{k^2}{\lambda_1^2} - \rho^2\left[\frac{k^2 + \beta^2(e-1)}{2k \sin k}\right]^2\left(1 + \frac{\sin 2k}{2k}\right) \quad (9a)$$

$$w_1(1) = \frac{\rho}{k^2}[k^2 + \beta^2(e-1)] \quad (9b)$$

$$w_1'(1) = \frac{\rho \cot k}{k}[k^2 + \beta^2(e-1)] \quad (9c)$$

Discussion of Equilibrium Eq. (8)

As mentioned previously, Eq. (8) is independent of condition (5d), $w_1(1) = \rho\xi_2(1)$, which serves only for determining the horizontal translation of the movable hinge. From a thorough discussion of the last equation, it was found[6] that for each slenderness ratio λ_I there is a maximum eccentricity e_{max} below which the frame buckles elastically losing its stability through a limit point; for loading eccentricities greater than e_{max}, the frame loses its stability through plastic buckling.

The derivation of nonlinear Eq. (8) is based on relations (7) and boundary condition (5e). It is worth observing that, in the case of linear stability theory, condition (5e) should be replaced by

$$w_2(1)=0 \tag{10}$$

By combining relations (7) and (10), it is found that

$$\frac{\rho(\beta^2-k^2)}{3\mu}+\frac{[k^2+\beta^2(e-1)]}{k\tan k}=0 \tag{11}$$

Apparently, from this nonlinear equation, one can obtain approximate solutions for equilibrium states of the frame, provided that $e\neq 0$. In case that $e=0$, it follows that either

$$\beta^2=k^2 \tag{12a}$$

or

$$k\tan k=3\mu/\rho \tag{12b}$$

Clearly, Eq. (12a), which yields $w_I'(1)=w_I(1)=0$, represents the fundamental equilibrium path, whereas the last equation corresponds to the secondary path. The intersection of these two paths gives the bifurcational critical load of the linear analysis. Note that the last buckling equation for $k=\beta$ coincides with that of linear stability analysis. In fact, Eqs. (6c) and (6d), by means of conditions (5f), (5k), (5l), and condition (10), lead to

$$C_I\left(\cos\beta-\frac{\rho\beta\sin\beta}{3\mu}\right)=\frac{\beta\rho^2 e}{3\mu},\ C_3=0,\ C_I=-C_3=C_I\frac{\beta}{2}\cos\beta \tag{13}$$

Obviously, for $e=0$ and $C_I\neq 0$, we find, again, the linear buckling equation. It is worth noticing that the axial displacement $\xi_I(x_I)$, determined by Eq. (6a), consists of two component parts. The first part, which is linear with respect to k^2, represents the shortening of the centerline of the column due to axial compression. The second part of the axial displacement (i.e., the integral) is due to bending of the column centerline and is nonlinear with respect to k^2. The last two terms in the equilibrium Eq. (8) evidently correspond to the foregoing two components of the axial displacement. It can be proved that the magnitudes of these two terms are considerably smaller than those of the other two terms of Eq. (8). On the basis of this observation, under certain conditions, either one of these terms can be omitted. Apparently, a considerable simplification of Eq. (8) is obtained by neglecting the nonlinear (integral) term in the axial displacement $\xi_I(x)$ given by Eq. (6a). On the other hand, the linear term in the axial displacement can be neglected in the case of large values of the length ratio ρ and/or large values of the slenderness ratio λ_I [see Eq. (8)].

In view of the foregoing development, one can establish a simplified nonlinear stability analysis which is associated with the following kinematic continuity conditions

$$w_2(1)=\frac{1}{\rho}\frac{k^2}{\lambda_I^2} \tag{14a}$$

$$w_2(1)=-\frac{1}{2\rho}\int_0^1 w_I'^2\,dx_I \tag{14b}$$

Subsequently, it is deduced that condition (14b) is valid only for large values of ρ and/or λ_I, whereas condition (14a) holds practically for all values of λ_I and/or ρ.

Simplified Nonlinear Analysis

On the basis of Eqs. (4) and (5g), the following differential equations governing the lateral deflection of the frame are established

$$w_I'''' + k^2 w_I''=0 \tag{15a}$$

$$w_2''''=0 \tag{15b}$$

The boundary conditions associated with these equations are

$$w_I(0)=w_2(0)=w_I''(0)=w_2''(0)=0 \tag{16a-d}$$

$$w_I'(1)=w_2'(1) \tag{16e}$$

$$w_I''(1)+(\mu/\rho)w_2''(1)+\beta^2\rho e=0 \tag{16f}$$

$$w_I'''(1)+k^2 w_I'(1)=0 \tag{16g}$$

$$(\beta^2-k^2)\rho^2+\mu w_2'''(1)=0 \tag{16h}$$

and

$$w_2(1)=\frac{k^2}{\rho\lambda_I^2} \tag{17a}$$

practically for all values of λ_I and/or ρ

$$w_2(1)=-\frac{1}{2\rho}\int_0^1 w_I'^2\,dx \tag{17b}$$

for large values of ρ and/or λ_I. It is to be noted that Eqs. (15) and (16) are also valid in the case of linear stability analysis with the exception that conditions (16h) and conditions (17) should be replaced, as mentioned previously, by the boundary condition $w_2(1)=0$. Integration of Eqs. (15), by means of the boundary conditions (16), yields Eqs. (6c-d) and, subsequently, relations (7). The kinematic continuity conditions (17a) and (17b), by virtue of relations (7), lead to the following two variants of the nonlinear equilibrium equation (8)

$$\frac{\rho(\beta^2-k^2)}{3\mu}+\frac{[k^2+\beta^2(e-1)]}{k\tan k}-\frac{k^2}{\rho^2\lambda_I^2}=0 \tag{18a}$$

and

$$\frac{\rho(\beta^2-k^2)}{3\mu}+\frac{[k^2+\beta^2(e-1)]}{k\tan k}-\left[\frac{k^2+\beta^2(e-1)}{2k\sin k}\right]^2\times\left(1+\frac{\sin 2k}{2k}\right)=0 \tag{18b}$$

It is worth noting that Eq. (18a), which includes the effect of the slenderness ratio λ_I, can be easily solved. The second equation is more complicated and is valid for large values of ρ and/or λ_I. Both equations are associated with limit point instability. However, Eq. (18b) for $e=0$ obviously yields $\beta^2=k^2$ and, therefore, is associated with bifurcational instability.

By using either Eq. (18a) or (18b), in conjunction with relations (9), one can establish the three displacement components of the joint at every level of the external loading β^2 and for various values of the parameters λ_I, μ, ρ, and e.

Direct Evaluation of Critical Loads

Nonlinear equilibrium equation (8), as well as either one of its variants, can be written in the form

$$F(k;\beta)=0 \tag{19}$$

This equation can be solved, at least implicitly, leading to

$$\beta=\beta(k) \tag{20}$$

Substituting $\beta(k)$ into Eq. (19) yields the identity

$$F[k,\beta(k)]\equiv 0 \tag{21}$$

which upon differentiation gives

$$F_k+F_\beta\frac{d\beta}{dk}=0$$

or

$$\frac{d\beta}{dk}=-\frac{F_k}{F_\beta} \qquad (F_\beta\neq 0) \tag{22}$$

The limit point load corresponds to a maximum of the curve β-k and, therefore, a necessary condition for its evaluation is

$$\frac{d\beta}{dk}=0 \text{ or } F_k(k,\beta)=0 \tag{23}$$

Thus, the critical load is obtained by solving the system of equations

$$F(k,\beta)=0, \qquad F_k(k,\beta)=0 \tag{24}$$

The solution (k_{cr},β_{cr}) of this system corresponds to the limit point which can be viewed as the point of intersection of the two curves given in Eq. (24). Since we are looking for a maximum, $d^2\beta/dk^2<0$ or, by means of relation (22)

$$F_{kk}(k_{cr},\beta_{cr})>0 \tag{25}$$

Note also that β_{cr} is the smallest load for which the system of Eq. (24) is fulfilled.

The equations $F_k(k,\beta)=0$ corresponding to Eqs. (8) and (18a) and (18b) are

$$\left[\frac{k^2+\beta^2(e-1)}{k^2\sin k}\right]^2\left[\frac{3k\sin k}{4}+\frac{3\sin k\sin 2k}{8}+\frac{k^2\cos k}{2}\right] -\frac{1}{2}\left[\frac{k^2+\beta^2(e-1)}{k^2\sin k}\right](2k+\sin 2k)+2\cos k -\left(\frac{1}{\rho^2\lambda^2}+\frac{\rho}{3\mu}\right)2k\sin k=0 \tag{26}$$

$$-\frac{1}{2}\left[\frac{k^2+\beta^2(e-1)}{k^2\sin k}\right)(2k+\sin 2k)+2\cos k -\left(\frac{1}{\rho^2\lambda^2}+\frac{\rho}{3\mu}\right)2k\sin k=0 \tag{27}$$

$$\left[\frac{k^2+\beta^2(e-1)}{k^2\sin k}\right]^2\left[\frac{3k\sin k}{4}+\frac{3\sin k\sin 2k}{8}+\frac{k^2\cos k}{2}\right] -\left[\frac{k^2+\beta^2(e-1)}{k^2\sin k}\right](2k+\sin 2k)+2\cos k-2k\frac{\rho}{3\mu}\sin k=0 \tag{28}$$

Condition (23) and its equivalent expressions, Eqs. (26), (27), and (28), together with condition (25), define stability criteria. Note that Eq. (26) was also derived using a perturbation technique.[6]

Table 1 Critical loads and displacements for $e=0$, $\mu=I_2/I_1=1$, and various values of λ_1 and ρ

		Nonlinear Eq. (8)			Simplified Eq. (18a)			Simplified Eq. (18b)		
λ_1	$\rho=\ell_2/\ell_1$	β^2_{cr}	$w_1(1)\times 10^{-2}$	$w_1'(1)\times 10^{-2}$	β^2_{cr}	$w_1(1)\times 10^{-2}$	$w_1'(1)\times 10^{-2}$	β^2_{cr}	$w_1(1)\times 10^{-2}$	$w_1'(1)\times 10^{-2}$
	0.25	1.515997	2.48290	0.90340	1.602739	3.00600	0.91181	2.10395	0	0
40	1	1.324893	2.30521	1.15485	1.341898	2.81794	1.38331	1.42196	0	0
	4	0.588045	1.56022	1.24050	0.589311	1.91066	1.51775	0.594996	0	0
	0.25	1.784471	1.30947	0.36151	1.837117	1.59360	0.38322	The results of the three last columns of Table 1 corresponding to $\lambda_1=40$ are the same for $\lambda_1=80$ and $\lambda_1=120$.		
80	1	1.372494	1.16710	0.56915	1.381363	1.42802	0.68896			
	4	0.591509	0.78292	0.62177	0.592115	0.95763	0.76021			
	0.25	1.88490	0.88828	0.21677	1.922326	1.08296	0.23715			
120	1	1.388771	0.78124	0.37745	1.394768	0.95641	0.45873			
	4	0.592669	0.52096	0.41358	0.593094	0.63946	0.50752			

Table 2 Critical loads and displacements for $e=-0.0025$, $\mu=I_2/I_1=1$, and various values of λ_1 and ρ

		Nonlinear Eq. (8)			Simplified Eq. (18a)			Simplified Eq. (18b)		
λ_1	$\rho=\ell_2/\ell_1$	β^2_{cr}	$w_1(1)\times 10^{-2}$	$w_1'(1)\times 10^{-2}$	β^2_{cr}	$w_1(1)\times 10^{-2}$	$w_1'(1)\times 10^{-2}$	β^2_{cr}	$w_1(1)\times 10^{-2}$	$w_1'(1)\times 10^{-2}$
	0.25	1.507664	2.50611	0.91546	1.594774	3.03385	0.92323	2.001874	0.39159	0.08046
40	1	1.274888	3.47330	1.78535	1.299690	4.24210	2.11736	1.308805	2.64940	1.33631
	4	0.533506	13.96220	11.28240	0.543951	17.06271	13.69292	0.53384	13.88740	11.22070
	0.25	1.768803	1.36021	0.38029	1.823054	1.65493	0.40173	The results of the three last columns corresponding to $\lambda_1=40$ are the same for $\lambda_1=80$ and $\lambda_1=120$.		
80	1	1.299279	2.88041	1.46059	1.320175	3.51896	1.74048			
	4	0.533758	13.90209	11.23293	0.544163	16.99181	13.63531			
	0.25	1.862511	0.96513	0.24085	1.902743	1.17600	0.26167			
120	1	1.304460	2.75444	1.39268	1.324512	3.36565	1.66146			
	4	0.533804	13.89467	11.22675	0.544202	16.97902	13.62491			

Numerical Results

In this section a comparison of numerical solutions based on Eq. (8) and each one of its variants given in relations (18a) and (18b) is presented. These solutions cover a relatively large range of values of the parameters λ_l, ρ, μ, and e. The solution of the three nonlinear equilibrium equations is performed by employing the Newton-Raphson numerical scheme. Once the solution, for each level of the nondimensionalized load β^2 is obtained, the corresponding equilibrium paths are presented by graphs of the load β^2 vs one of the joint displacement components, evaluated by means of relations (9). The critical load β^2_{cr} is obtained either as the maximum (limit point) load in the foregoing graphs, or by a direct evaluation through the systems of two equations, i.e., Eqs. (8) and (26), (18a) and (27), or (18b) and (28). The results presented herein are given in both graphical and tabular form. From Tables 1-3 one can study the individual and coupling effect of the parameters e, μ, ρ, and λ_l upon the critical loads and critical displacements by using the accurate nonlinear analysis as well as its two approximate variants.

From Table 1, established for $e=0$ and $\mu=1$, one can see that Eq. (18a) compared with the accurate one [Eq. (8)] gives very reliable results for all values of λ_l and ρ. In the worst case, the critical load is not greater than 5.7% of the accurate one. Also, in all cases the critical displacements are greater (i.e., on the safety side) than the corresponding ones of the nonlinear analysis. Equation (18b) is associated with bifurcational instability and always yields the same results regardless of the value of the slenderness ratio λ_l. However, for $\rho>1$ the last equation leads to good estimations for the critical loads which are not on the safety side. In this case, the major discrepancy from the accurate analysis is less than 7.5%. The critical displacements obtained by Eq. (18b) are zero, because $\beta^2=k^2$ (bifurcational instability). In conclusion, the more simplified Eq. (18a) is clearly, in all cases, more efficient than Eq. (18b).

From Table 2, computed for $e=-0.0025$ and $\mu=1$, one can observe that both Eqs. (18a) and (18b) are associated with limit point instability. Moreover, it should be noted that Eq. (18b) for $\rho>1$ and $\lambda_l>40$ gives very precise critical loads and, in any event, better than those of Eq. (18a). However, the critical displacements obtained by Eq. (18b) for $\rho<4$ and all λ_l are always smaller (and, therefore, not on the safety side) than the corresponding displacements obtained by Eqs. (8) and (18a). Nevertheless (in the worst case), the major discrepancy of Eq. (18a) regarding the evaluation of critical loads is less than 6%. The critical displacements obtained by the last equation are always greater (i.e., on the safety side) than those of the nonlinear analysis. These advantages render Eq. (18a) more convenient for application than Eq. (18b).

From Table 3, computed for $e=-0.0025$, one can see the influence of the parameter $\mu=I_2/I_l$ upon the critical loads evaluated in Table 2. A first observation is that the critical load increases as μ increases. Moreover, for $\rho>1$ and $\mu>1$, Eq. (18b) gives better results than those of the simpler Eq. (18a). This effect is more pronounced as the slenderness ratio λ_l increases. However, the discrepancy between the nonlinear analysis and its simplified variant given by Eq. (18a), in the worst case, is less than 6.0%. Thus, Eq. (18a), in view of its simplicity, must be considered as more suitable for practical applications than Eq. (18b).

In Fig. 2 a typical plot of the nonlinear equilibrium path, β^2 vs $w_l'(1)$, for $e=0$, $\lambda=40$, and $\rho=\mu=1$, is shown; this is established on the basis of the nonlinear buckling equation (8) as well as its two variants given in relations (18a) and (18b). Note that the last equation, when $e=0$, implies bifurcational instability. Finally, it is to be noted that Eq. (18a) is associated with linear differential equations and linear boundary conditions.

From the foregoing discussion, it is clear that the approximate nonlinear analysis associated with Eq. (18a), due to its simplicity and reliability for establishing critical loads and

Table 3 Critical loads for $e=-0.0025$ and various values of λ_l, μ, and ρ

λ_l	μ	ρ	Nonlinear Eq. (8) β^2_{cr}	Simplified Eq. (18a) β^2_{cr}	Simplified Eq. (18b) β^2_{cr}
		0.25	1.061199	1.115313	1.308805
	0.25	1	0.528720	0.539914	0.533842
		4	0.156682	0.160013	0.156709
		0.25	1.507664	1.594774	2.001874
40	1	1	1.274888	1.299690	1.308805
		4	0.533506	0.543951	0.533804
		0.25	1.678081	1.778206	2.304464
	4	1	1.908792	1.941694	2.001874
		4	1.306336	1.326082	1.308805
		0.25	1.206883	1.241992	The results of the above column corresponding to $\lambda_l=40$ are the same for $\lambda_l=80$ and $\lambda_l=120$.
	0.25	1	0.532514	0.543115	
		4	0.156702	0.160030	
		0.25	1.768803	1.823054	
80	1	1	1.299279	1.320175	
		4	0.533758	0.544163	
		0.25	1.987179	2.048679	
	4	1	1.971302	1.993890	
		4	1.308182	1.327624	
		0.25	1.253897	1.281974	
	0.25	1	0.533247	0.543733	
		4	0.156706	0.160033	
		0.25	1.862511	1.902743	
120	1	1	1.304460	1.324512	
		4	0.533804	0.544202	
		0.25	2.101783	2.146085	
	4	1	1.987163	2.007060	
		4	1.308527	1.327913	

equilibrium paths, is very efficient for structural design purposes.

Conclusions

The most important conclusions of this investigation are summarized as follows:

1) Two simplified nonlinear buckling analyses, based on the assumption of small axial strains, moderate rotations, and slightly modified kinematic continuity conditions, are presented. The governing differential equations and the associated boundary conditions of these analyses are those of the linear buckling analysis, with the unique exception that the kinematic continuity conditions referring to the joint lateral displacements are slightly modified. More specifically, in the modified condition (which is a simplified version of the corresponding nonlinear kinematic condition), the translational displacement of the joint is due either to bending of the bar axis (considered as incompressible) or to its shortening under the axial compression.

2) The range of applicability of both simplified nonlinear buckling analyses is established through a thorough parametric study for a large variety of values of all parameters (i.e., length and moment of inertia ratios, slenderness ratio, and loading eccentricity). The simplified buckling analysis, which neglects the joint axial component due to bending of the bar axis, is extremely simple, fast, reliable for practical applications, and very efficient for frames with a large number of joints. The critical loads and critical displacements obtained by this approximate nonlinear buckling analysis are always slightly greater than those derived by the accurate nonlinear buckling analysis.

3) Simple criteria for establishing the limit of stability leading to a direct determination of critical loads, obtained either by the accurate or the simplified buckling analyses, are also presented.

4) The study of the individual and coupling effect of the aforementioned parameters upon the load-carrying capacity of the frame is a by-product of this investigation.

References

[1]Bleich, F., *Buckling Strength of Metal Structures*, McGraw-Hill Book Co., New York, 1952.

[2]Hutchinson, J. R. and Koiter, W. T., "Post-buckling Theory," *Applied Mechanics Review*, Vol. 23, 1970, pp. 1353-1366.

[3]Brush, D. O. and Almroth, B. O., *Buckling of Bars, Plates and Shells*, McGraw-Hill Book Co., New York, 1975.

[4]Koiter, W. T., "On the Stability of Elastic Equilibrium," thesis presented to the Polytechnic Institute of Delft, the Netherlands, 1945, in partial fulfillment of the requirements for the degree of Doctor of Philosophy; English translation, NASA TT-F-10833, 1967.

[5]Kounadis, A. N., Giri, J., and Simitses, G. J., "Nonlinear Stability Analysis of an Eccentrically Loaded Two-Bar Frame," *Journal of Applied Mechanics*, Vol. 44, Series E, No. 4, 1977, pp. 701-706.

[6]Simitses, G. J. and Kounadis, A. N., "Buckling of Imperfect Rigid-Jointed Frames," *Journal of Engineering Mechanics*, Div. ASCE, EM3, 1978, pp. 569-586.

[7]Vlahinos, A. S. and Kounadis, A. N., "Nonlinear Elastic Limit State Analysis of Rigid Jointed Frames," *International Journal of Nonlinear Mechanics*, Vol. 16, No. 314, 1981, pp. 379-385.